MSW MANAGEMENT -Multidisciplinary, Scientific Work and Management Journal
ISSN: 1053-7899
Vol. 36 Issue 2, 2026, Pages 2461-2467

Thermogravimetric and Fourier-Transform Infrared Spectroscopic Characterization of Tread and Reinforced Rubber Compounds in Commercial Electric Bicycle Tires

H. Gerengi[1], Doğaç Çağıl[2], Gasim Altundal[3*]
[1]*Department of Mechanical Engineering, Düzce University, Düzce, Türkiye*
[2]*Anlas Tyre Company R&D Center, Düzce, Türkiye*
[3]*Anlas Tyre Company R&D Center, Düzce, Türkiye*
husnugerengi@duzce.edu.tr; dogac.cagil@anlas.com.tr; gasim.altundal@anlas.com.tr
[1] https://orcid.org/0000-0002-9663-4264; [2] https://orcid.org/0009-0006-9565-8527; [3] https://orcid.org/0000-0002-8856-4737;
**Corresponding author:* gasim.altundal@anlas.com.tr

Abstract— *The electric bicycle (e-bike) market is growing and demands tires with better puncture resistance, improved wet and dry grip, and optimized rolling resistance. A comparative characterization of the tread (black) and reinforced-layer (colored) rubber compounds from three leading commercial e-bike tire brands, referred to as Sample A, Sample B, and Sample C, was performed using thermogravimetric analysis per ASTM D6370 and Fourier-transform infrared spectroscopy. TGA decomposition profiles were used to quantify the volatile matter and fractions of polymer, carbon black, and inorganic filler, whereas FTIR fingerprint analysis was used to determine the base polymer types. All three tread compounds utilize an NR/SBR blend; however, substantial filler loading difference (carbon black from 6.9 to 30.4 wt.% and inorganic matter from 16.9 to 20.5 wt.%) with hardness varying between 57 and 75 Shore A reveals different design philosophies among these products. The reinforced-layer compounds showed even greater compositional diversity where Sample A used pure NR with low filler, while Sample B contained a high inorganic filler content of 36.3 wt.%. The FTIR spectra could clearly differentiate between NR-only compounds and those containing an SBR blend based on the presence or absence of certain absorption bands for aromatic C–H and phenyl rings. These results can be used as a quantitative benchmark for the development of next-generation reinforced e-bike tire compounds.*

Keywords: ***Electric bicycle tire; TGA; FTIR; rubber compound***

I. INTRODUCTION

The global electric bicycle market has grown rapidly over the last decade due to urbanization, environmental awareness, and battery technology improvements [1]. E-bikes are not the same as conventional bicycles; they put much greater loads on tires because of heavier frames, motor-assisted torque, and higher cruising speeds. Together, these factors accelerate tread wear and increase the risk of a puncture [2]. Therefore, developing tires that provide better puncture resistance, good wet and dry grip, reasonable rolling resistance, and long tread life is an important engineering challenge [3].

The performance properties of a rubber tire are mainly determined by its compound formulation [4]. The polymer matrix is usually natural rubber (NR), styrene–butadiene rubber (SBR), or their blends that control the baseline viscoelastic behaviour. Reinforcing fillers like carbon black and precipitated silica control hardness, abrasion resistance, and hysteresis loss [5]. A complete quantitative knowledge of competitor formulations is a prerequisite before starting to design any new optimized tire compound.

Thermogravimetric analysis is a widely used and effective method for the reverse engineering of rubber compounds. It can measure mass loss as a function of temperature under controlled atmospheres to allow quantification in one experiment of volatile content, polymer fraction, carbon black loading, and inorganic residue [6]. Fourier-transform infrared spectroscopy helps TGA by providing qualitative identification of the polymer types and functional groups present. Characteristic absorption bands in the fingerprint region allow very quick differentiation between NR, SBR, and other elastomers [7].

In this paper, we show an organized comparative characterization using TGA and FTIR along with complementary hardness, density, and ash content measurements for both tread and reinforced-layer compounds from three commercially available e-bike tire brands.

II. MATERIALS AND METHODS

A. Sample Preparation

Three commercially available e-bike tires were procured: Sample A, Sample B, and Sample C. Each tire was dissected to separate the tread compound (black layer) from the sub-tread reinforced compound (colored layer). The reinforced layers were identified by color: green (A), red (B), and purple (C) (Fig. 1). Specimens were conditioned at 23 ± 2 °C and 50 ± 5% RH for 24 hours prior to analysis.

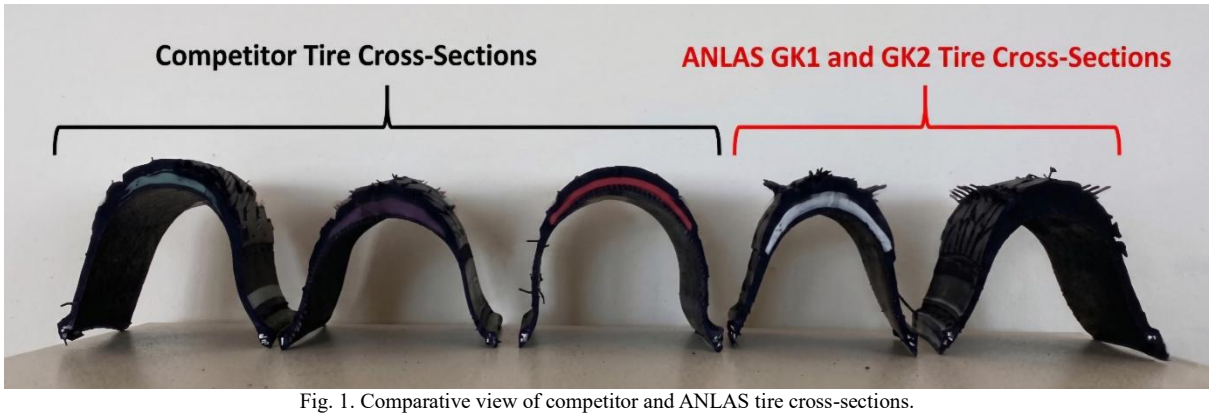

Fig. 1. Comparative view of competitor and ANLAS tire cross-sections.

B. Thermogravimetric Analysis (TGA)

TGA was performed according to ASTM D6370. Specimens (~10–15 mg) were heated from ambient to 1000 °C at 20 °C/min under nitrogen (up to ~500–550 °C), then switched to air to oxidize carbon black. Residue at 1000 °C represents inorganic fillers. Simultaneous DTA was recorded.

C. Fourier-Transform Infrared Spectroscopy (FTIR)

FTIR analysis was conducted using an ATR accessory. Spectra were collected over 4000–400 cm^{-1} at 4 cm^{-1} resolution with 32 co-added scans. NR was identified by the C=C stretching near 1660 cm^{-1} and the =C–H out-of-plane bending near 835 cm^{-1}. SBR was confirmed by aromatic C–H stretching near 3025 cm^{-1} and mono-substituted phenyl ring vibrations at 699 and 760 cm^{-1} [8].

D. Complementary Characterization

Shore A hardness, density by hydrostatic immersion, and ash content at 550 °C were measured as complementary tests.

III. RESULTS AND DISCUSSION

A. FTIR Polymer Identification–Tread Compounds

FTIR analysis of the tread compounds confirmed that all three brands employed an NR/SBR blend as the polymer matrix. The simultaneous presence of isoprene-related C=C stretching (1660 cm^{-1}), strong =C–H out-of-plane bending at 835 cm^{-1} characteristic for NR, and aromatic C–H stretching near 3025 cm^{-1} together with phenyl ring absorption at 699 cm^{-1} diagnostic for SBR clearly indicated the presence of NR and SBR phases in each specimen [9]. Individual FTIR spectra are shown in Figure 2 while a comparative overlay is provided in Figure 3.

MSW MANAGEMENT -Multidisciplinary, Scientific Work and Management Journal
ISSN: 1053-7899
Vol. 36 Issue 2, 2026, Pages 2456-2460

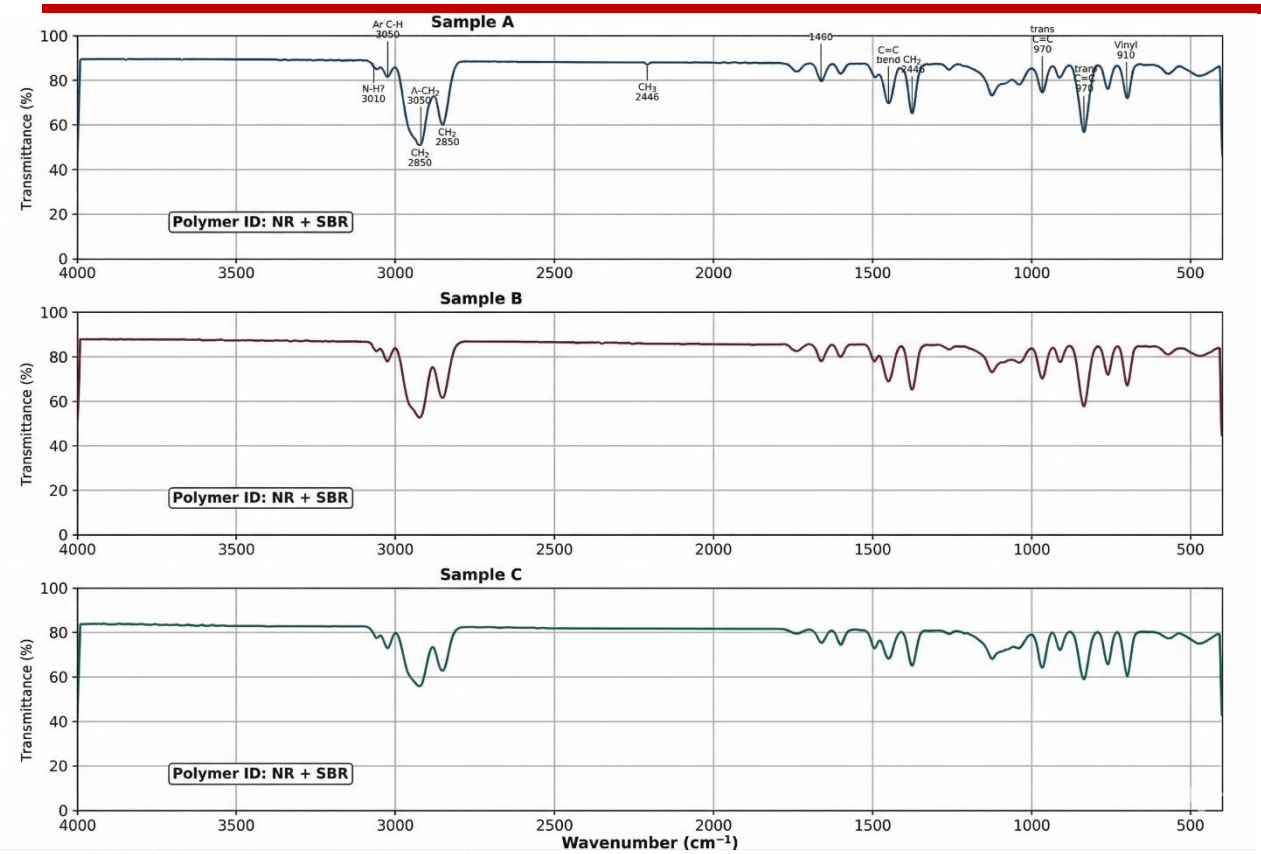

Fig. 2. Individual FTIR-ATR spectra of the three tread compounds with key peak assignments.

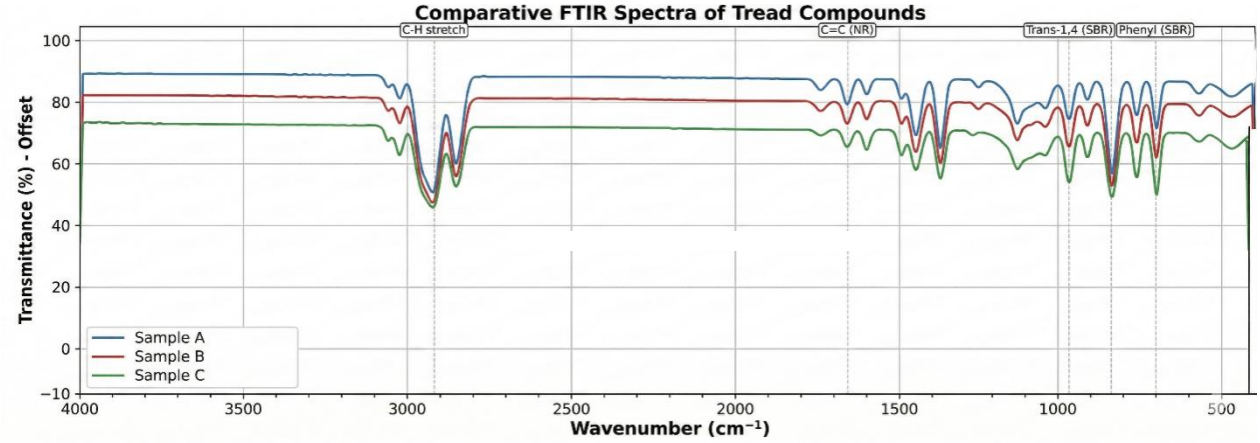

Fig. 3. Comparative FTIR overlay of the three tread compounds showing consistent NR/SBR fingerprint.

B. FTIR Polymer Identification – Reinforced-Layer Compounds

The reinforced-layer compounds exhibited greater polymer diversity. Sample A utilized pure NR, as evidenced by the complete absence of the aromatic C–H stretching band near 3025 cm^{-1} and the phenyl ring absorption at 699 cm^{-1} in its spectrum (Figure 4, top panel). In contrast, samples B and C retained the NR/SBR blend. The spectrum of sample B also showed a pronounced broad absorption near 1100 cm^{-1}, consistent with Si–O stretching of silicate-based filler, in agreement with its exceptionally high inorganic content (36.3 wt.%). Figure 5 presents the comparative overlay.

MSW MANAGEMENT -Multidisciplinary, Scientific Work and Management Journal
ISSN: 1053-7899
Vol. 36 Issue 2, 2026, Pages 2456-2460

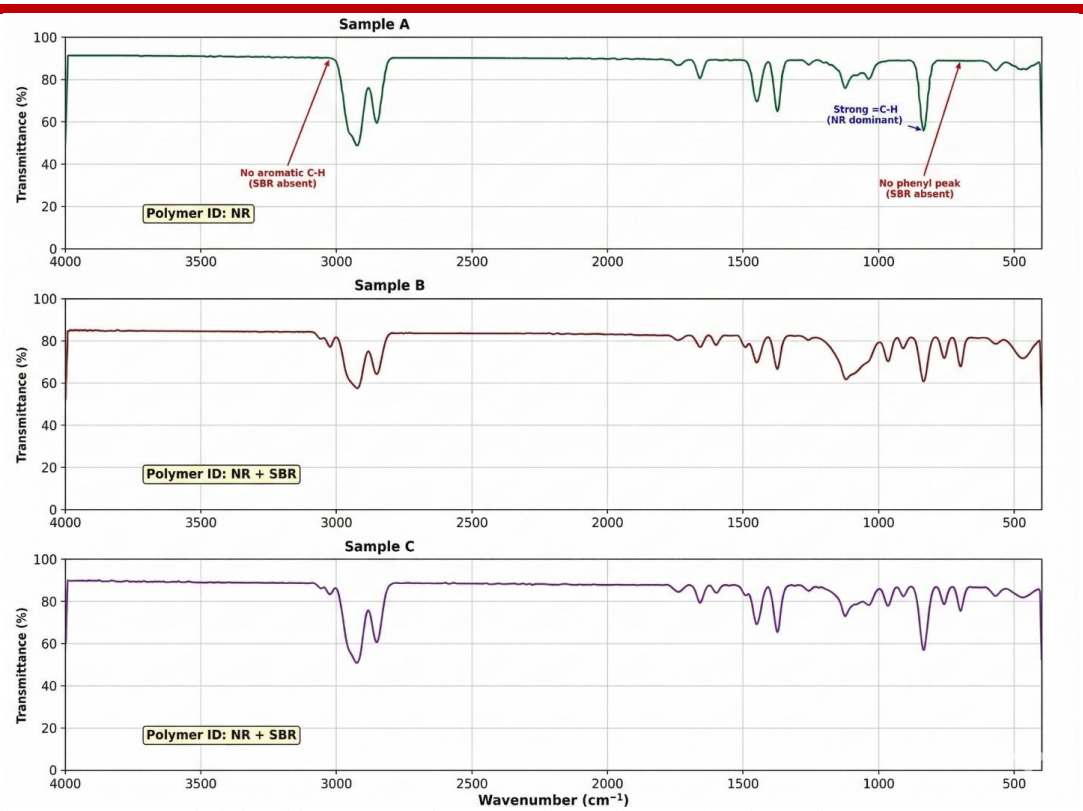

Fig. 4. Individual FTIR-ATR spectra of reinforced-layer compounds. Note the absence of SBR markers in Sample A.

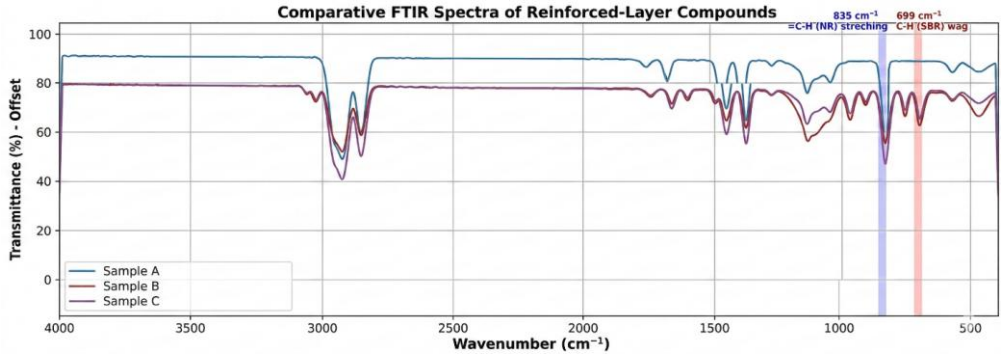

Fig. 5. Comparative FTIR overlay of reinforced-layer compounds highlighting polymer differences

C. FTIR fingerprint region analysis

A detailed comparison of the fingerprint region (1800-600 cm^{-1}) is presented in Figure 6. In the tread compounds (upper panel), all three spectra exhibit matching peak positions for NR (1660, 1375, 835 cm^{-1}) and SBR (966, 760, 699 cm^{-1}) markers, with intensity variations reflecting differences in polymer ratios and filler content. The key differentiating feature in the reinforced-layer compounds (lower panel) is the complete absence of the 699 and 760 cm^{-1} phenyl peaks in Sample A, definitively confirming the pure NR formulation. The prominent Si–O absorption near 1100 cm^{-1} in Sample B indicates substantial silicate-based filler usage.

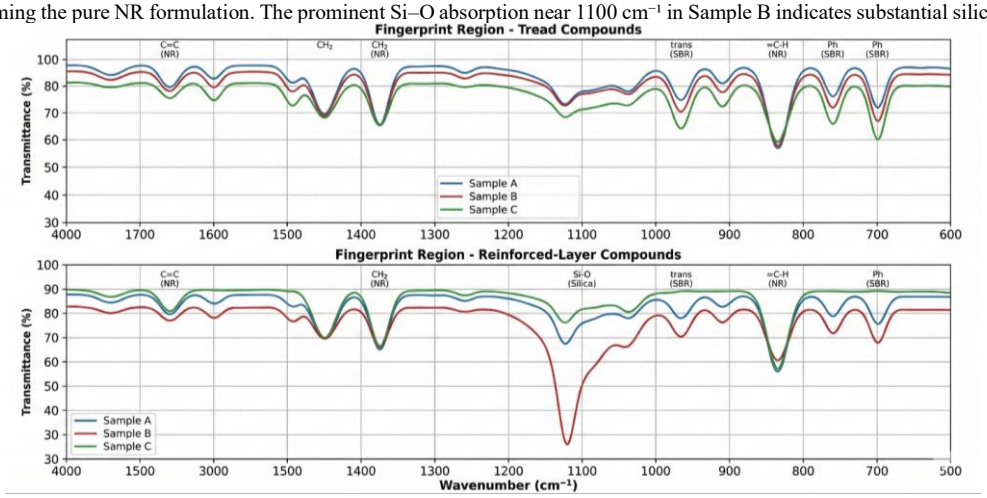

Fig. 6. FTIR fingerprint region (1800–600 cm^{-1}) comparison: tread (top) and reinforced-layer (bottom) compounds.

MSW MANAGEMENT -Multidisciplinary, Scientific Work and Management Journal
ISSN: 1053-7899
Vol. 36 Issue 2, 2026, Pages 2456-2460

D. TGA of Tread Compounds

Representative TGA/DTA thermograms are presented in Figures 7–9, and a comparative overlay is presented in Figure 10 (Table 1). Each curve exhibits multi-step decomposition: gradual mass loss below 300 °C (volatiles/plasticizers), major polymer degradation between 300°C and 550°C, and carbon black oxidation near 600°C–700°C upon air switching.

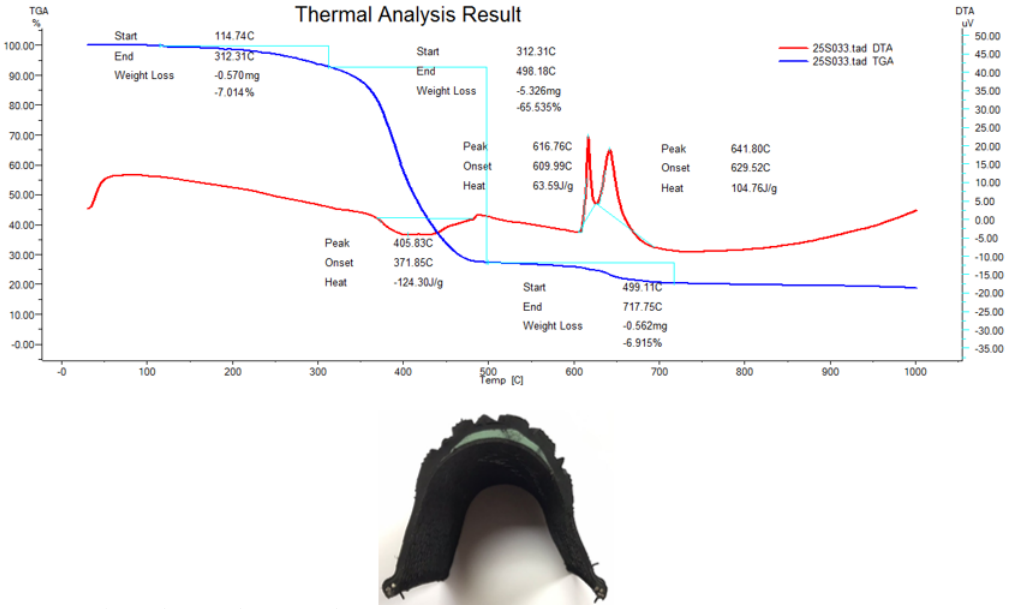

Fig. 7. TGA/DTA thermogram of Sample A tread compound.

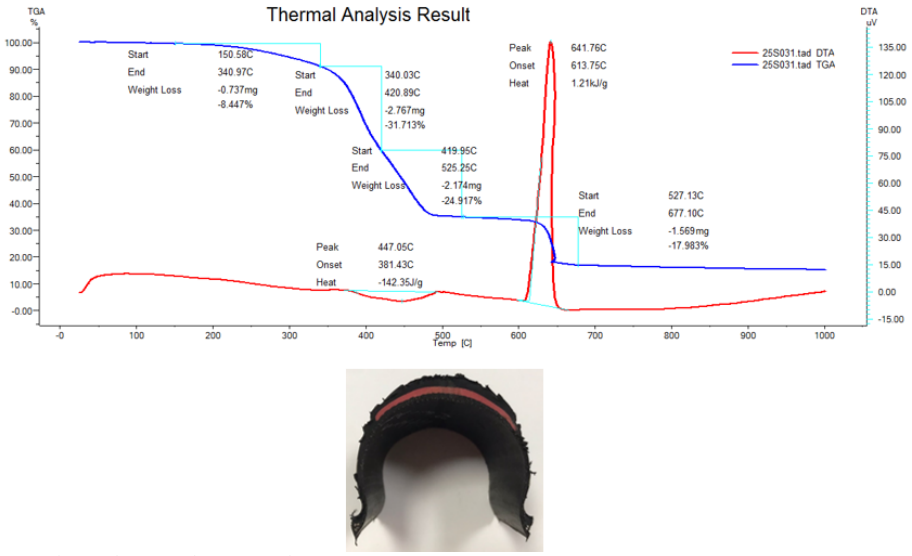

Fig. 8. TGA/DTA thermogram of Sample B tread compound.

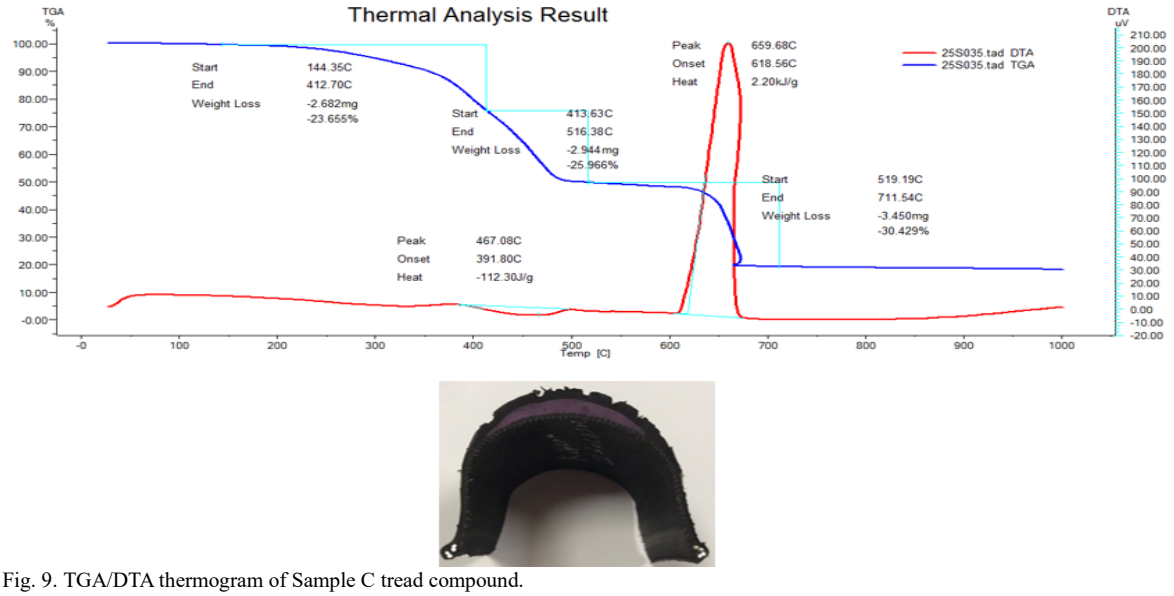

Fig. 9. TGA/DTA thermogram of Sample C tread compound.

MSW MANAGEMENT -Multidisciplinary, Scientific Work and Management Journal
ISSN: 1053-7899
Vol. 36 Issue 2, 2026, Pages 2456-2460

Sample A had the highest volatile and polymer content (72.5 wt.%) and the lowest carbon black (6.9 wt.%), indicating that it was a soft formulation. Sample C had the lowest polymer fraction (49.6 wt.%) and most carbon black (30.4 wt.%), resulting in a 74-75 Shore A hardness. Sample B was in between the two extremes.

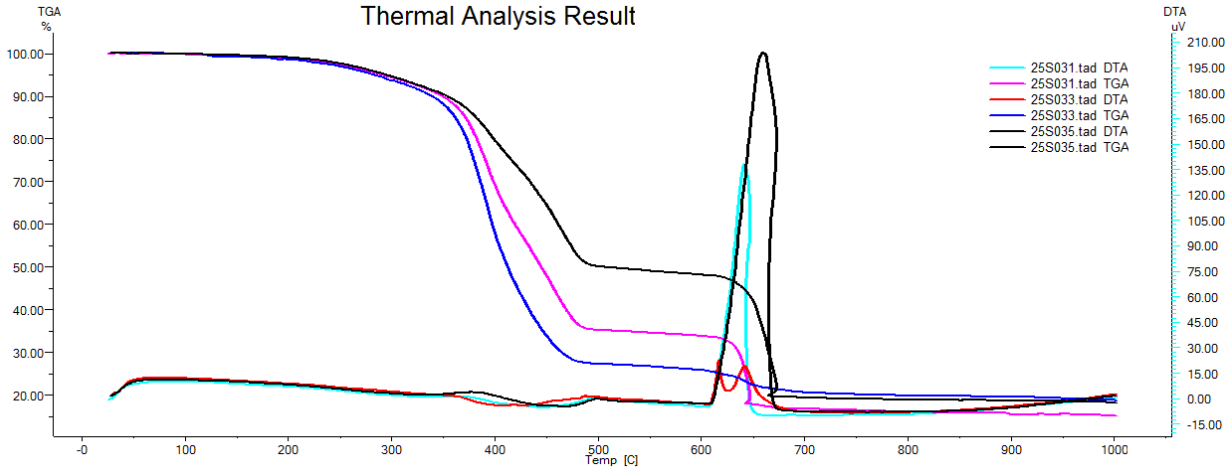

Fig. 10. Comparative TGA/DTA overlay of the three tread compounds.

TABLE I
COMPREHENSIVE CHARACTERIZATION OF THE TREAD COMPOUNDS.

Parameter	Unit	Sample A	Sample B	Sample C
FTIR Polymer ID	—	NR + SBR	NR + SBR	NR + SBR
Volatile Matter and Polymer	wt.%	72.549	65.09	49.621
Carbon Black	wt.%	6.915	17.98	30.429
Inorganic Matter	wt.%	20.536	16.93	19.95
Ash Content	wt.%	22.2	18.92	20.7
Density	g/cm³	1.102	1.132	1.268
Hardness	Shore A	57–58	60–61	74–75

E. TGA of Reinforced-Layer Compounds

Figures 11–13 show individual TGA/DTA thermograms for the reinforced compounds, with the comparative overlay in Figure 14 (Table 2).

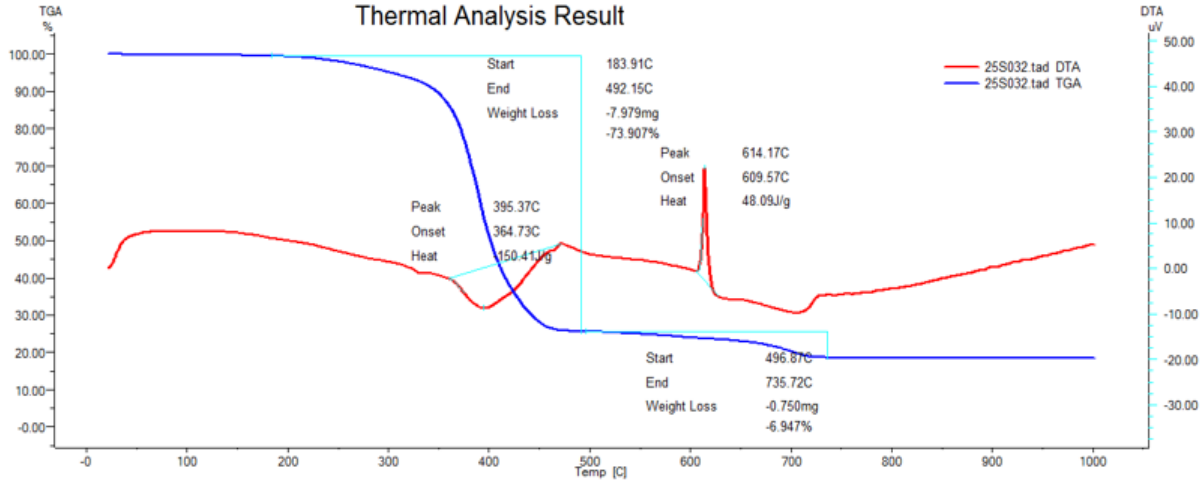

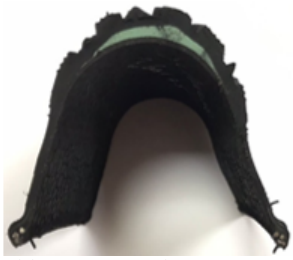

Fig. 11. TGA/DTA thermogram of Sample A reinforced-layer compound.

MSW MANAGEMENT -Multidisciplinary, Scientific Work and Management Journal
ISSN: 1053-7899
Vol. 36 Issue 2, 2026, Pages 2456-2460

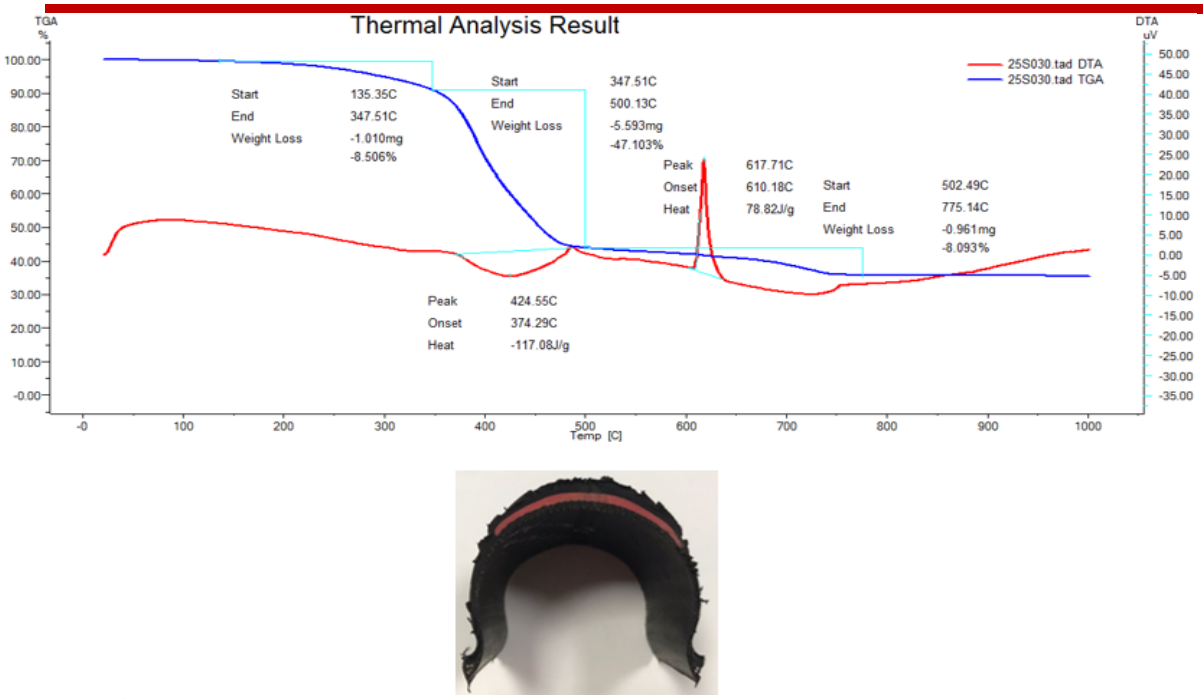

Fig. 12. TGA/DTA thermogram of Sample B reinforced-layer compound.

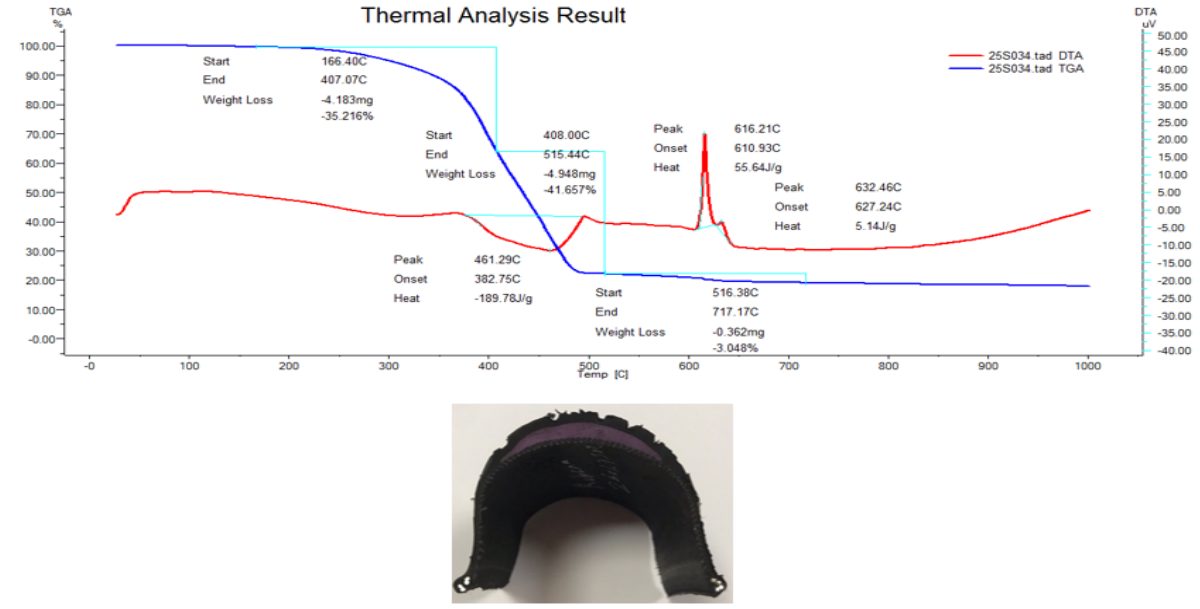

Fig. 13. TGA/DTA thermogram of Sample C reinforced-layer compound.

Sample C exhibited the highest volatile/polymer content (76.9 wt.%), followed by Sample A (73.9 wt.%), while Sample B contained only 55.6 wt.%, compensated by a remarkably high inorganic filler loading of 36.3 wt.%.

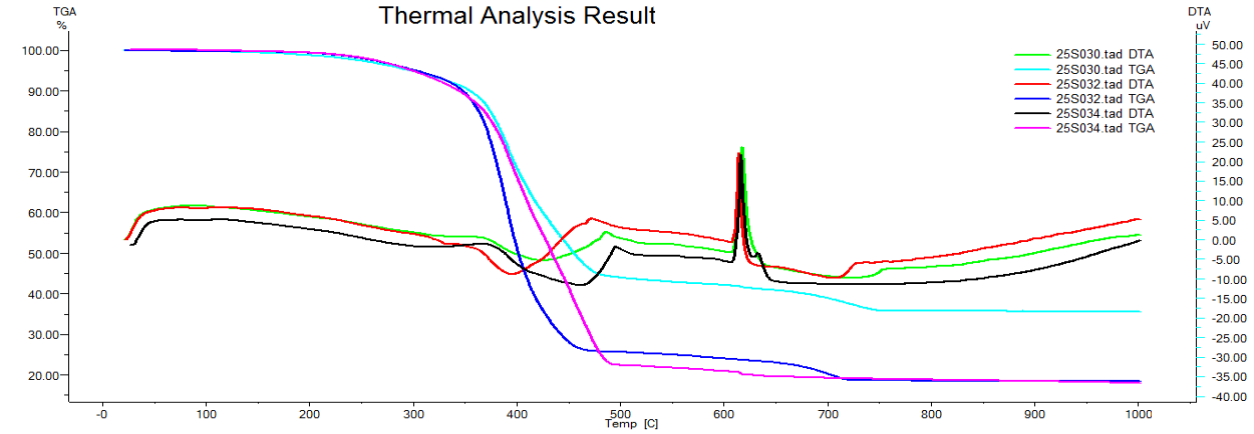

Fig. 14. Comparative TGA/DTA overlay of reinforced-layer compounds.

MSW MANAGEMENT -Multidisciplinary, Scientific Work and Management Journal
ISSN: 1053-7899
Vol. 36 Issue 2, 2026, Pages 2456-2460

TABLE IIIII
COMPREHENSIVE CHARACTERIZATION OF REINFORCED-LAYER COMPOUNDS

Parameter	Unit	Sample A	Sample B	Sample C
FTIR Polymer ID	—	NR	NR + SBR	NR + SBR
Volatile Matter and Polymer	wt.%	73.90	55.61	76.873
Carbon Black	wt.%	6.94	8.10	3.048
Inorganic Matter	wt.%	19.16	36.29	20.079
Ash Content	wt.%	20.37	35.65	21.43
Density	g/cm³	1.096	1.256	1.107
Hardness	Shore A	52–53	58–59	59–60

F. Comparative Discussion

The DTA curves presented in Figures 7–14 provide valuable insights into the thermal events accompanying the decomposition of the rubber compounds. In all thermograms, a distinct exothermic peak observed between approximately 350 °C and 500 °C corresponds to the thermal oxidative degradation of the polymer matrix (NR/SBR or pure NR). Following the switch to an oxidizing atmosphere at around 550–600 °C, a second sharp exothermic peak appears, which is attributed to the combustion of carbon black. Notably, the reinforced-layer compound of Sample B (Figure 12) exhibits a more pronounced exothermic feature in the polymer degradation region compared to the others; this may be associated with catalytic effects arising from its exceptionally high inorganic filler content (36.3 wt.%), likely comprising silicate-based materials. Additionally, minor endothermic dips below 200 °C are detectable in some samples, indicating the volatilization of processing oils, plasticizers, or other low-molecular-weight additives. Overall, the DTA profiles are fully consistent with the mass loss steps recorded by TGA and corroborate the compositional differences among the samples, particularly the elevated filler loading in Sample B and the distinct polymer formulation of Sample A's reinforced layer.

The combined TGA and FTIR results reveal three fundamentally different design strategies. Sample A adopts a soft-tread, high-polymer approach with minimal carbon black and pure NR in the reinforced layer to achieve superior ride comfort and flexibility. Sample B employs moderate carbon black in the tread paired with an exceptionally heavily filled reinforced layer (36.3 wt.% inorganic filler), creating a stiff puncture-protection barrier. Sample C pursues aggressive reinforcement at the tread level (30.4 wt.% carbon black, 74–75 Shore A), while its reinforced layer contains the highest polymer content (76.9 wt.%) and lowest carbon black (3.0 wt.%).

The FTIR spectra provided critical complementary information that TGA alone could not provide. While TGA quantified the mass fractions of organic and inorganic components, FTIR clearly indicated the specific polymer types employed in each layer, revealing that Sample A's reinforced layer uses a fundamentally different polymer strategy (pure NR) compared to Sample B and Sample C (NR/SBR blend). The ash content measurements consistently corroborated the TGA inorganic residue data with discrepancies of less than 2 percentage points.

IV. Conclusions

Three different brands of e-bike tires were used in a systematic study using TGA and FTIR to characterize tread and reinforced-layer rubber compounds. The major findings are: All tread compounds use NR/SBR blends, as confirmed by FTIR through the simultaneous presence of NR markers (835, 1660 cm^{-1}) and SBR markers (699, 966 cm^{-1}). The reinforced-layer polymers Sample A uses pure NR (confirmed by the absence of aromatic peaks) while Sample B and Sample C retain NR/SBR.

Carbon black loading in the tread differed from 6.9 wt.% for Sample A to 30.4 wt.% for Sample C with hardness ranging from 57 to 75 Shore A. More variation was seen in the composition of reinforced layers where Sample B had a very high inorganic filler content at 36.3 wt.%.

The integration of TGA compositional information with FTIR polymer identification creates an all-inclusive reverse engineering approach toward developing advanced materials for next-generation e-bike tires. Further research will be directed at improved formulations that seek an ideal compromise among puncture resistance, rolling resistance, and ride comfort.

Acknowledgement

This study was funded by TÜBİTAK-1505 (Project Number 5240109) through the Support Program for University-Industry Collaboration. The authors express their gratitude to Anlaş Anadolu Lastik Sanayi ve Ticaret A. Ş. for their partnership and extend their thanks to Canan Yüksel, Emine Demir, and Beyza Aşıkoğlu for their assistance in preparing the samples. This scientific study was presented at the International Conference on Green and Sustainable Chemistry (ICGASC-26), organized by the Association for Scientific and Academic Research (ASAR), held on May 2026, Paris, France

References

[1] Rodgers, B., & Waddell, W. H. (2013). Tire engineering. In J. E. Mark, B. Erman, & C. M. Roland (Eds.), *The science and technology of rubber* (4th ed., pp. 619–665). Academic Press. https://doi.org/10.1016/B978-0-12-394584-6.00014-5

[2] Aggarwal, A., Hackel, N., Grunert, F., Ilisch, S., Beiner, M., & Blume, A. (2024). Investigation of rheological, mechanical, and viscoelastic properties of silica-filled SSBR and BR model compounds. *Polymers*, 16(22), 3212. https://doi.org/10.3390/polym16223212

[3] Demir, E., Altundal, G., Gerengi, H., & Yüksel, C. (2023). Investigation of the potential of using liquid rubbers in rubber industry. *Journal of Materials Science and Chemical Engineering, 11*, 21–30. https://doi.org/10.4236/msce.2023.119002

[4] Demir, E., Gerengi, H., Savcı, K., Altundal, G., Yüksel, C., & Çağıl, D. (2024). Exploration of green alternatives to 6PPD (P-phenylenediamine) used as antiozonant and antioxidant in the rubber industry. *Materials Sciences and Applications, 15*(4), 87–100. https://doi.org/10.4236/msa.2024.154007

[5] Altundal, G., Gerengi, H., Savcı, K., Demir, E., Yüksel, C., & Çağıl, D. (2024). Evaluation of nylon 6 and nylon 66 cord fabrics for scooter tyre production under different curing conditions. *Materials Sciences and Applications, 15*(10), 464–474. https://doi.org/10.4236/msa.2024.1510031

[6] Altundal, G., Gerengi, H., Çetin, E., Kapcak, U., & Kaymaz, K. (2020). Performans bisiklet lastiği sırt karışımının geliştirilmesi ve özelliklerinin incelenmesi. *Düzce Üniversitesi Bilim ve Teknoloji Dergisi, 8*, 1661–1675. https://doi.org/10.29130/dubited.698101

[7] Çetin, E., Gerengi, H. (2025). Exploring hazelnut shell-derived carbon as an eco-friendly additive in bicycle tire manufacturing. *Materials and Technology, 59*(1), 133–141. https://doi.org/10.17222/mit.2024.1315

[8] Hummel, D. (1959). The infrared spectroscopic identification of rubber before and after cure to the soft and hard rubber states. *Rubber Chemistry and Technology, 32*(3), 854–869. https://doi.org/10.5254/1.3542454

[9] Azevedo, J. B., Oliveira, G. E., & Ferreira, M. (2018). Quantification of elastomer blends by FT-IR spectroscopy. *Polímeros, 28*(5), 447–455. https://doi.org/10.1590/0104-1428.08317